ORIGINAL ARTICLE

A. V. Minakov · M. I. Pryazhnikov · V. A. Zhigarev ·
V. Y. Rudyak · S. A. Filimonov

Numerical study of the mechanisms of enhanced oil recovery using nanosuspensions

Abstract The results of the numerical study of oil recovery enhancement using nanosuspension are presented. The research was carried out using the volume of fluid method (VOF) for a 2D microporous core model. Experimentally measured values of interfacial tension (IFT) and the contact angle (CA) were used for numerical modeling. An aqueous suspension with silicon oxide nanoparticles (5 nm) is used. It was shown that when 1 wt% of nanoparticles are added to the displacing liquid, its density increases by about 1%, the viscosity increases by 10%, the IFT decreases by 10%, and the contact angle increases from 70 to 145°. The results of numerical study showed that the injection of nanoparticles has a significant effect on the displacement front movement in the microporous model. It has been shown that the nanosuspension can increase the oil recovery factor (ORF) almost twice as compared to water. To clarify the mechanisms of increasing the oil recovery during the reservoir flooding with nanofluid, a systematic study of factors affecting the displacement process efficiency was carried out. Viscosity, interfacial tension and the wetting angle of the displacing fluid were considered as such factors. As a result of systematic research, it has been shown that the main factor affecting the increase in the oil recovery flooding of nanosuspensions is a variation of wettability.

1 Introduction

From a practical standpoint, the problem of studying two-phase flows in microchannels is extremely relevant to the development of enhanced oil recovery technology. It is known that 78% of gas and 58% of all proven world oil reserves are in the so-called terrigenous (sand) reservoirs. In such a reservoir, the rock is a porous medium composed of sand particles with a grain size of 0.01 to 10 mm, while the void space is filled with oil-bearing fluid. In this case, the void space is essentially an extensive network of microchannels with characteristic sizes ranged from 1 to $1000 \mu m$, through which the movement of a multiphase (oil–gas–water) medium occurs. One of the most common methods to develop such deposits is reservoir flooding by water or surfactant solutions. However, the efficiency of oil recovery is currently low. The average oil recovery factor ranges from 15 to 55%. Therefore, the increase in the oil recovery factor is very important.

Today, the following methods of increasing oil recovery are actively used: flooding with chemical reagents (acids, alkalis, solutions of polymers and surfactants), gas displacement (injection of CO_2 and other gases) and thermal methods (injection of steam or supercritical fluids and in situ combustion) [7,17,19,20]. These

A. V. Minakov (✉)· M. I. Pryazhnikov · V. A. Zhigarev · V. Y. Rudyak · S. A. Filimonov
Siberian Federal University, Krasnoyarsk, Russia
E-mail: tov-andrey@yandex.ru

A. V. Minakov · M. I. Pryazhnikov · S. A. Filimonov
Kutateladze Institute of Thermophysics, SB RAS, Novosibirsk, Russia

processes increase oil recovery through different mechanisms such as lowering interfacial tensions, wettability alteration and rheological modification. The processes have been utilized to increase well production rates of hydrocarbons to commercial levels to enable oil industries to optimize the upstream production capacity to meet up with increasing energy demand.

The search for alternative technologies is being intensively conducted. In recent years, there have been works showing that the use of nanosuspensions allows increasing significantly the ORF from the reservoir [2,4,10,14,15,18]. A summary of these studies is shown in Table 1.

Thus, in [14], SiO2 nanoparticles were used for this purpose. As a result, it was shown that the use of nanofluid allows increasing the ORF from 40 to 70% compared to water. The authors of work explained this effect by the fact that due to nanoparticle adsorption, the rock material acquires the water wetting properties.

In the paper [2], TiO2 nanosuspensions were used for oil recovery. The results of measurements have shown that when using nanosuspension, the oil displacement factor increases at least 1.3-fold. Mcelfres et al. [10] also received a very high increase in oil recovery from the injection of the 10 wt% silica nanosuspension (4–20 nm). They showed that the ORF increases by 22%. Similar values of increasing the oil recovery factor when using nanosuspensions were obtained in the work [18]. It used metal nanoparticles (150 nm) at a very low concentration (0.001%). No detailed explanation of this significant effect has been provided. Hu *et al.* 2016 in the paper [4] obtained a significant increase in the oil recovery factor (33%) using nanosuspension with rutile ellipsoid TiO2 nanoparticles (with a diameter of approximately 150 nm and aspect ratio in the range of 7-9) at extremely low concentrations of 20 ppm.

One of the reasons why surfactant solutions are used in oil recovery enhancing technologies is a change in the wettability of the rock, contributing to the better displacement of oil. In recent years, quite a large number of laboratory experiments have been conducted, confirming the high efficiency of nanosuspensions to reduce the contact angle on the surface of various rocks [5,8,15].

For example, the paper [15] describes studies on alteration in the contact angle by SiO_2 nanoparticles. It was shown that the contact angle for oil in water was 140 degrees, and after adding nanoparticles to water, the contact angle decreased to 50 degrees. Thus, the addition of nanoparticles led to a complete change in the type of wettability. An even more significant effect on wettability when using nanofluid with particles of zirconium oxide (24 nm) was obtained in the paper [5]. The contact angle has decreased from 180 to 32 degrees. In a two-phase flow experiments, Li et al. [8] investigated the effect of concentration on wettability using crude oil against silica nanofluids with various concentrations. Among their findings was that the increase in concentration increased wettability.

Experiments conducted in recent years have shown that the wetting angle is not the only indicator of the nanoparticle efficiency in relation to the washing off retained oil from the rock. It was found that in the nanosuspensions medium-specific phenomena occur on the contact surface of the oil with the rock, in contrast to the ordinary fluids not containing nanoparticles. Namely, thin wedges of nanofluid can spread along this surface, gradually forming a continuous film separating oil and rock. Experiments using nanoparticle suspensions are described in detail in [21].

Many potential mechanisms have been proposed to explain the effect of nanosuspensions on the ORF. The most important in consideration are: increase in the viscosity of displacing fluid, changing the wettability of the surface, reduction in interfacial surface tension and spreading of nanofluids on solids. Despite the considerable interest and quite a large number of experimental works on this topic, there is no definitive understanding of the mechanisms responsible for the enhancement of oil recovery by nanosuspensions during reservoir flooding. The physical processes considered during oil displacement are quite complex. Experimental studies alone are not enough to establish the mechanisms for increasing the oil recovery factor. For a deeper understanding, it is necessary to use numerical simulation.

In this regard, the present paper deals with comprehensive numerical study to clarify noted mechanisms.

2 Experimental study

In this paper, a computational study of the oil displacement from the microporous rock using nanofluid has been carried out. At that, correct numerical simulation requires data on the interfacial tension and the contact angle. To obtain these data, systematic experimental studies of interfacial tension and surface wettability in nanosuspension–oil–rock systems were carried out. Light oil (density—831 kg/m^3, viscosity—0.0078 Pa s) was used in the experiments.

Nanosuspensions were made from distilled water and SiO2 nanoparticles. The average particle size was measured using the DT1202 acoustic and electroacoustic analyzer. The average size SiO2 nanoparticles was

Table 1 Summary on the experimental study of nanofluid enhanced oil recovery (ORF)

Ref.	Type of nanoparticle (NP)	NP concentration, wt%	NP size, nm	ORF % Brine, water	Nanofluids (NF)	Efficiency of NF %
Roustaei and Bagherzadeh [14]	SiO$_2$	0.1-0.6	20–70	47	76	38
Ehtesabi et al. [2]	TiO$_2$	0.01	54 × 15 elongated	41	55	25
		0.05			51	20
Mcelfresh et al. [10]	SiO$_2$	0.01	21–40	55.61	58.25	4.5
		0.05		57.02	63.16	9.7
		0.1		62.23	62.23	0
Suleimanov et al. [18]	Nonferrous metal NPs	0.001	90–110	51	60.3	15
Hu et al. [4]	TiO$_2$	0.0005	150 ± 20 with aspect ratio 7-9	35.66	37.50	4.9
		0.001			41.86	8.3
				38.40	40.64	2.0
		0.002			39.72	6.6
				39.83	40.74	13
		0.005		37.09	40.94	22
		0.01		35.56		
		0.05		31.80		
Karimi et al. [5]	ZrO$_2$	0.05	24	5	63	92
Li et al. [8]	SiO$_2$	0.01	7	51.42	56.07	8.3
		0.05			67.02	7.9
		0.05		61.71	68.75	6.8
		0.1		64.06	54.79	7.8
				50.53		

Table 2 Viscosity coefficient and density of the nanosuspension with SiO2 nanoparticle

Nanoparticle mass concentration, %	Viscosity, mPa s	Density, g/cm^3
0.125	0.8964	0.9977
0.25	0.8976	0.9984
0.5	0.9113	0.9997
1	0.9836	1.0025
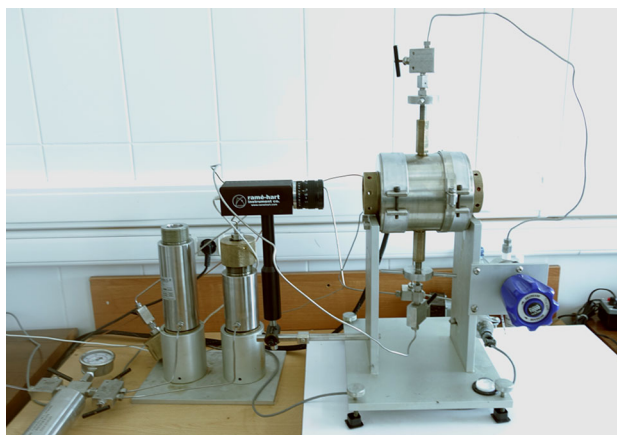
Fig. 1 Photograph of IFT-820-P automatic tensiometer

5 nm. The particle concentration ranged from 0.125 to 1 wt%. A two-step technique was used to prepare samples of nanofluids. To break down the nanoparticle conglomerates, the suspension was processed in an ultrasonic dispersant. The stability of the obtained suspension was investigated by the TurbiscanLAB analyzer and Rheolaser MASTER. It was shown that the studied nanosuspension was stable for ten days from the moment of preparation.

The study of the nanosuspension viscosity coefficient was carried out using OFITE HPHT rotary viscometer. The rotation speed range 3-600 rpm corresponded to the shear rate ranged from 5 to 1022 1/s. The viscosity measurement error was about 2%. The dependence of the nanosuspension viscosity coefficient on the nanoparticle concentration is given in Table 2. As you can see, with the addition of 1 wt% of nanoparticles, the viscosity increases by about 9%. A detailed study of the viscosity behavior of nanosuspensions can be found in our work [16].

Measurement of interfacial tension and wetting angle was taken by means of IFT-820-P automatic tensiometer (Fig. 1). A detailed description of the results of experiments on the effect of nanoparticles on wettability can be found in our recent work [13]. The operation principle of IFT-820-P tensiometer is based on the hanging drop method, in which the surface tension is determined through measurements of the geometric parameters of the drop of the investigated liquid. The measurement results were processed using the DropImage Advanced software. The final data were obtained by averaging over four independent measurements. The mean standard deviation in the experiments did not exceed 5%. The measuring method of the surface tension coefficient was tested on water and ethylene glycol. At that, good agreement with the reference data was obtained.

From the start, the effect of the concentration of nanoparticles on the interfacial tension of nanosuspension–oil was studied. Figures 2 and 3 show the measurement results for a nanofluid with SiO_2 particles (5 nm). As a consequence of the research, it was shown that with an increase in the nanoparticle concentration, the interfacial tension on the oil–nanosuspension interface changes weakly within a wide range of nanoparticle concentrations. The maximum reduction of IFT with the addition of nanoparticles was about 7%.

The study of the effect of nanoparticles addition on the contact angle, on the contrary, has shown a very significant dependence on the nanoparticle concentration. It has been shown that the nanomaterials significantly affect the oil wetting characteristics of the rock (Figs. 4, 5). Influence analysis of the nanoparticle additives on the wetting angle has shown that the wetting angle (internal) increases with increasing concentration of nanoparticles significantly, from 73 to 153°. Thus, it was found that the injection of nanoparticles to the liquid significantly worsens the wettability of the rock by oil. In fact, the addition of 1 wt% of nanoparticles to
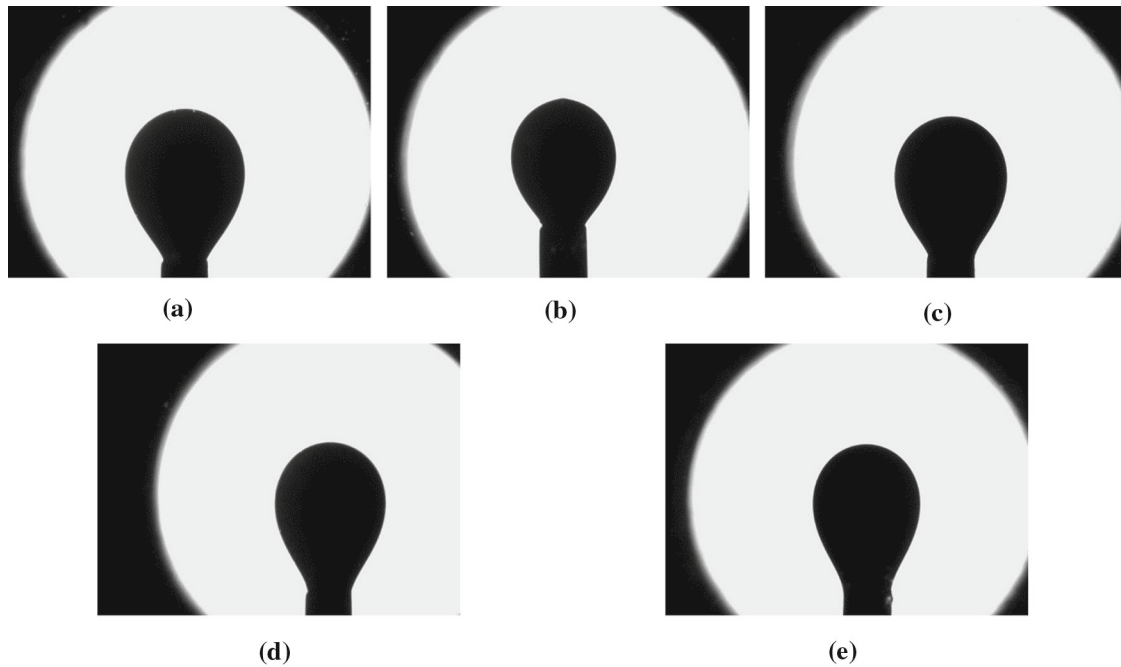
Fig. 2 Photographs of oil droplets in the SiO_2 nanosuspension at different nanoparticle concentrations: **a** 0%; **b** 0.125%; **c** 0.25%; **d** 0.5%; **e** 1%
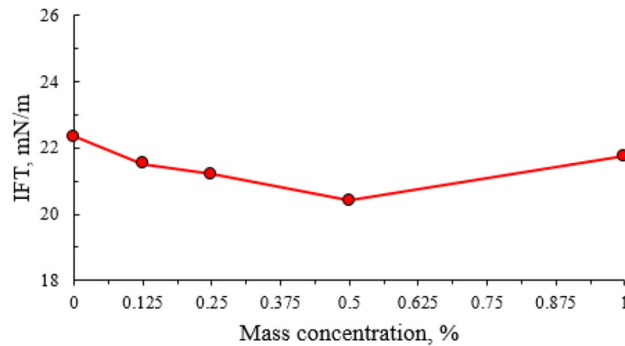

Fig. 3 Interfacial tension of nanosuspension–oil versus SiO_2 nanoparticle concentration

water makes core rock sample) nonwettable by the oil. The obtained experimental data on the viscosity, IFT coefficient and the CA of nanofluid were further used in systematic numerical investigation.

3 Mathematical model and numerical technique

Next, a systematic numerical study of the oil displacement from the porous rock using nanosuspensions was done. The VOF method [3,11,12] was used to simulate a two-phase flow in a porous medium. This model can simulate immiscible liquid–liquid multicomponent flow by solving the Navier–Stokes equations with the volume concentration of one of the phases. The model is introduced into consideration the volume fraction of the displacing fluid (nanosuspension) α and the volume fraction of the displaced fluids (oil) β. Since $\alpha + \beta = 1$, in the calculations it is sufficient to use only the volume fraction of the displacing fluid α.

In this case, the density and viscosity of the mixture included in the Navier–Stokes equations are determined as follows:

$$\rho = \rho_1(\varphi)\alpha + (1 - \alpha)\rho_2, \tag{1}$$

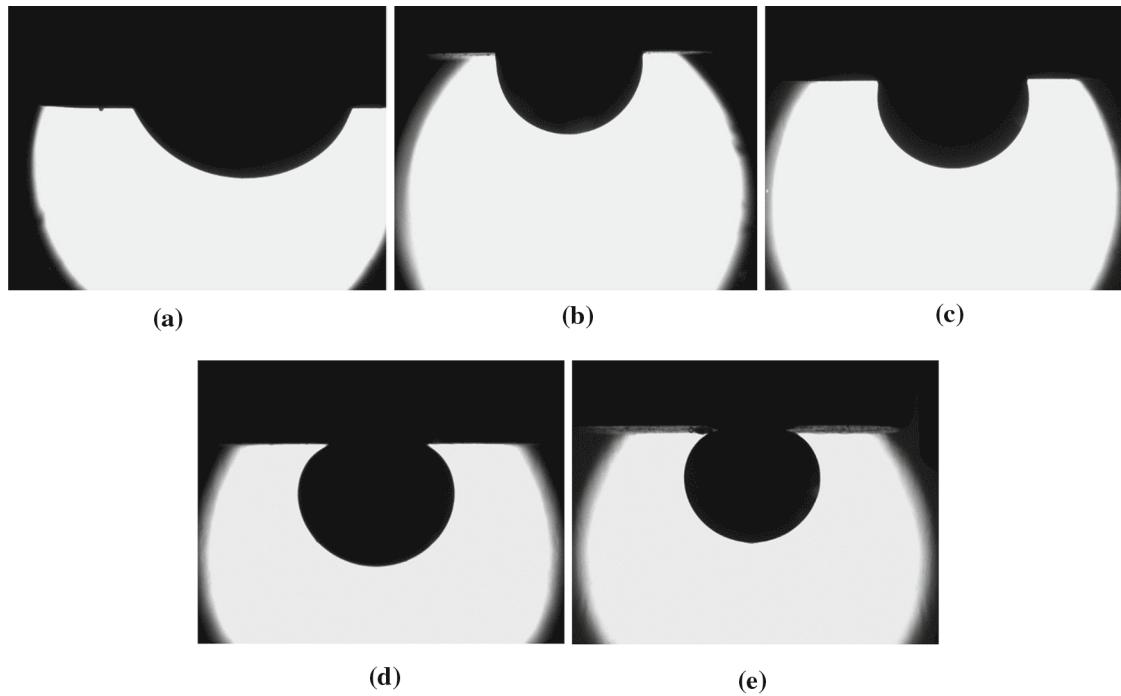$$\mu = \mu_1(\varphi)\alpha + (1 - \alpha)\mu_2. \tag{2}$$

Fig. 4 Photographs of oil droplets in SiO$_2$ nanosuspension on the surface of core at different nanoparticle concentrations: **a** 0%; **b** 0.125%; **c** 0.25%; **d** 0.5%; **e** 1%
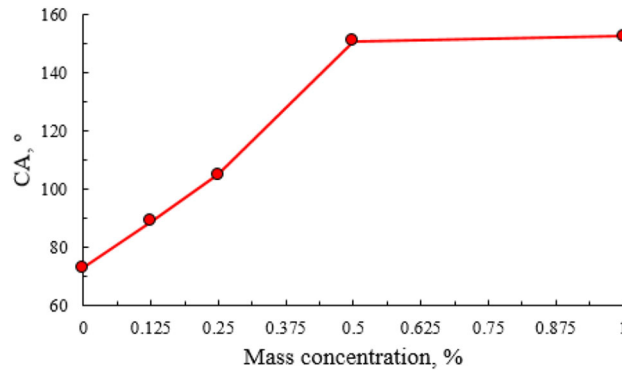

Fig. 5 Contact angle (CA) of nanosuspension–oil versus SiO$_2$ nanoparticle concentration

where ρ_2 and μ_2 are the density and viscosity of oil and $\rho_1(\varphi)$ and $\mu_1(\varphi)$ are the density and viscosity of nanofluids, respectively, depending on particle concentration φ (see Table 1).

The mass conservation equation in this case has a standard form:

$$\frac{d\rho}{dt} + \nabla(\rho \cdot \vec{V}) = 0. \tag{3}$$

Here $\vec{V}$ is mixture velocity, which is determined by solving the momentum equation:

$$\frac{\partial}{\partial t}\left(\rho\vec{V}\right) + \nabla \cdot \left(\rho\vec{V}\vec{V}\right) = -\nabla p + \nabla \cdot \left[\mu\left(\nabla\vec{V} + \nabla\vec{V}^T\right)\right] + \rho\vec{g} + \vec{F}_s, \tag{4}$$

where p denotes the static pressure of mixture, $\vec{g}$ denotes the gravitational force and $\vec{F}_s$ is the volume force vector caused by capillary forces.

To simulate the movement of the interface in the process of oil displacement, the following transfer equation is solved:

$$\frac{\partial \alpha}{\partial t} + \nabla \cdot \left(\alpha \vec{V} \right) = 0. \tag{5}$$

When oil is displaced from a porous medium, capillary forces are very important. To simulate surface tension, the continuum surface force (CSF) algorithm by Brackbill et al. [1] was used. For this method, surface tension effects are modeled by adding a source term in equations (4):

$$\vec{F}_s = \sigma\left(\varphi\right) k \nabla \alpha, \tag{6}$$

where $\sigma(\varphi)$ is the interfacial tension coefficient, k is the curvature of the oil–water interface, which is defined as:

$$k = \nabla \left(\frac{\vec{n}}{|\vec{n}|} \right), \tag{7}$$

where $\vec{n}$ is the normal vector to the interface between the phases, which is determined by the following in the volume of the computational domain:

$$\vec{n} = \nabla \alpha. \tag{8}$$

On the walls of the computational domain, the normal vector is determined using the following expression:

$$\vec{n} = \vec{n}_w cos\left(\theta\left(\varphi\right)\right) + \vec{\tau}_w sin\left(\theta\left(\varphi\right)\right), \tag{9}$$

where $\theta(\varphi)$ is contact angle at the wall, $\vec{n}_w$ is the unit vector normal to the wall and $\vec{\tau}_w$ is the unit vector tangential to the wall.

When taking into account the phenomenon of surface wettability, the dynamic behavior of the contact angle can play an important role [12]. According to [6,12] the dynamic contact angle θ_d is determined using the equilibrium value of the contact angle $\theta(\varphi)$ as follows:

$$\theta_d = f(Ca + f^{-1}\left(\theta\left(\varphi\right)\right)), \tag{10}$$

where f is the Hoffman function, f^{-1} is the inverse value of the Hoffman function:

$$f = \arccos \left\{ 1 - 2\tanh(5.16 \left(\frac{Ca + f^{-1}(\theta}{1 + 1.31(Ca + f^{-1}(\theta)^{0.99}} \right)^{0.706} \right\}, \tag{11}$$

where $Ca = \frac{\mu U}{\sigma(\varphi)}$ is capillary number and U is the velocity of oil–water interface nearest to the wall mesh cells, which is found as: $U = (\vec{n} \cdot \vec{V})$.

In the calculations, experimentally measured values of the viscosity $\mu(\varphi)$, density $\rho(\varphi)$, interfacial tension $\sigma(\varphi)$ and contact angle $\theta(\varphi)$ of nanosuspension depending on particle concentration φ were used. These data are given in Sect. 2.

It should be noted that in this work we used hydrophilic nanoparticles. This excludes the transport of nanoparticles through the interface between the aqueous phase and oil. In the case of using nanoparticles with mixed wettability, such a transport is probably possible. To simulation this process, it is possible to use the algorithm proposed in the work [9] or other algorithms that take into account the slip of velocities.

The numeric technique used in this paper and results of its testing is described in detail in the papers [11,12]. To solve the system of nonlinear differential equations (3–5), we used the FVM (finite volume method). The coupling between the velocity field and pressure is realized using the SIMPLEC (Semi-Implicit Method for Pressure Linked Equations-Consistent) algorithm. The PRESTO (PREssure STaggering Option) scheme for calculation continuity balance was used. An implicit second-order scheme was used to approximate the unsteady terms of the transport equations. A second-order central-difference scheme was used to approximate the convective terms of the Navier–Stokes equations. A total variation diminishing (TVD) scheme with high-resolution interface capturing (HRIC) limiter was used to solve the transport equation (5).

The following settings were used in the simulation. A two-dimensional digital porous micromodel was created to simulate the displacement process. The main characteristics of sandstone (Berea Sandstone^{TM}
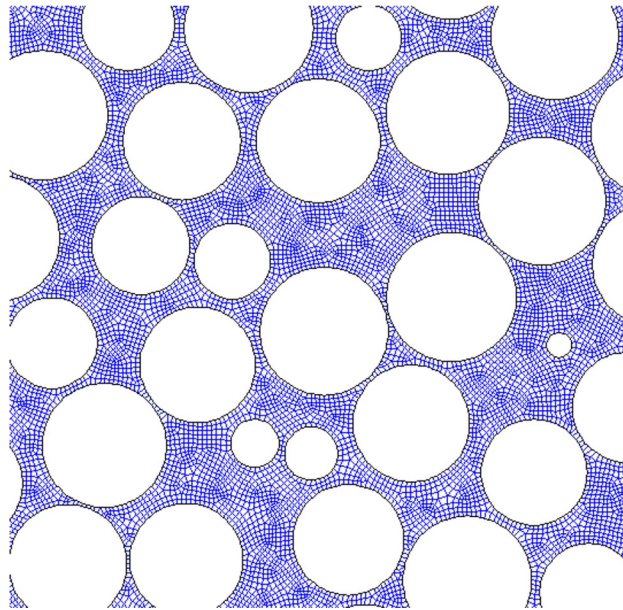
Fig. 6 Fragment of the calculation grid

Table 3 Study of the computational mesh detailing

The number of mesh cells	Final value of ORF
320000	0.372
786000	0.331
1428000	0.327

samples) were used in this rock model. The porosity of model -30%, the average grain diameter $-100\,\mu$m. The porous medium in this model was formed as a random filling of circles with an average size of 100 microns. The computational domain was a rectangle with a width of 1.5 mm and a height of 2 mm. At the upper boundary of the computational domain, the inlet boundary conditions were set with a fixed value of the volume flow rate (10 ml/min) of displacing fluid. This corresponded to the standard conditions of the experiments for the core flooding. At the lower boundary, the free outlet boundary conditions were set with a fixed value of the static pressure equal to zero. Symmetry boundary conditions were set on the sidewalls.

At the initial instant, the computational micromodel was 100% saturated with oil. In the course of simulation, the displacing fluid filled the micromodel, displacing the oil. As a result of calculations, the value of the ORF and the pressure loss were determined.

A series of methodological calculations was performed to study the influence of detailing the computational mesh and other numerical parameters on the results of numerical modeling. The results of calculating the displacement of oil by water on grids with different numbers of cells are shown in Table 3. Thus, for the final calculations, a mesh with about 0.8 million cells was chosen (see Fig. 6). The value of the time step was determined from the condition CFL < 2 (Courant–Friedrichs–Lewy number).

4 Simulation results

First, the influence of nanosuspension concentration on the efficiency of oil displacement was studied. To do this, a series of calculations were carried out in which the particle concentration varied from 0 to 1 wt%. Figures 7, 8 and 9 illustrate the oil displacement process by nanosuspension.

The simulation results show that the injection of nanoparticles to the fluid significantly affects the oil displacement from the micromodel. In the case of pure base fluid or nanofluid with a low concentration of nanoparticles, the displacing agent moves through the oil in the form of individual rivulets or trickles. Such rivulets quickly breakthrough to the micromodel outlet. This is clearly seen in Fig. 8. After that, the water
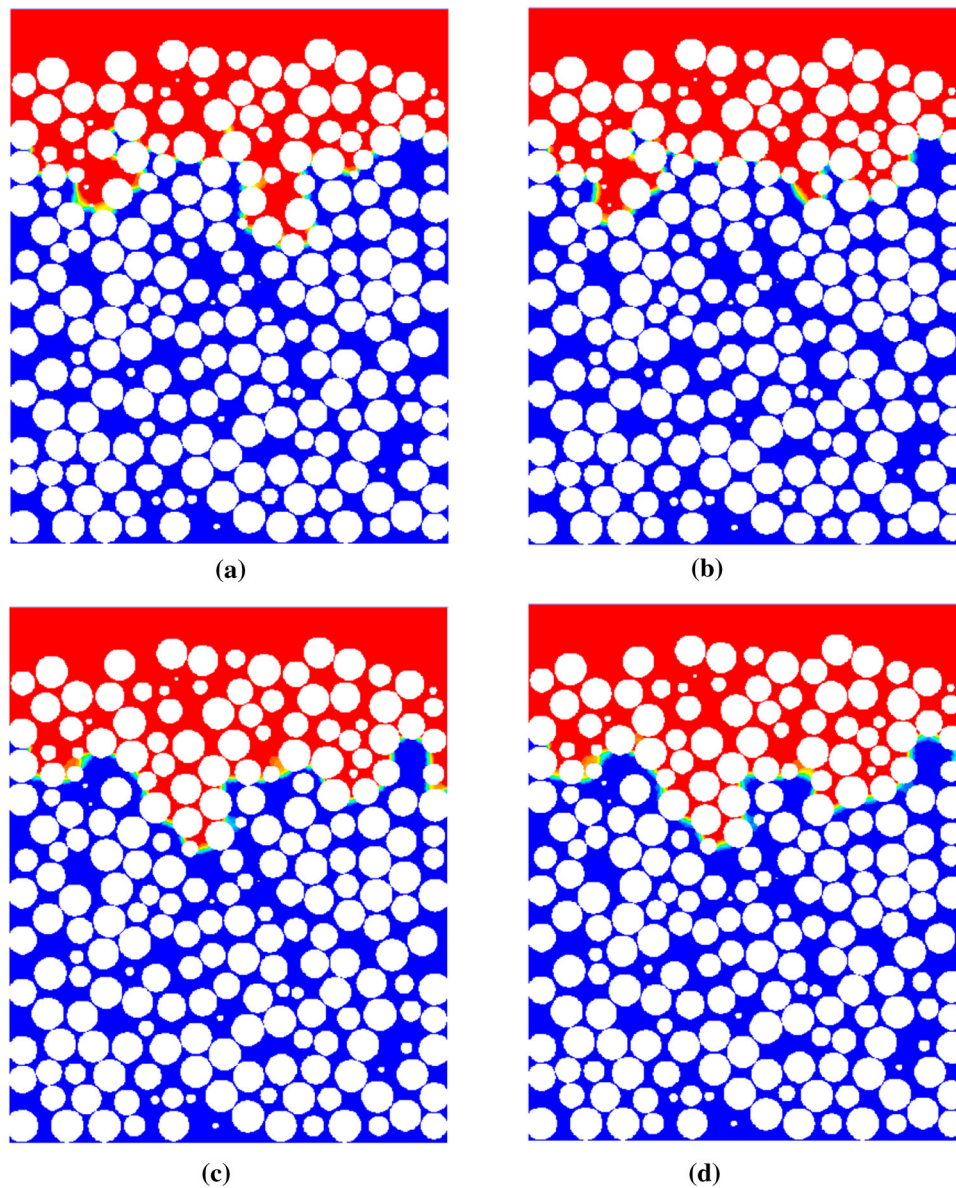
Fig. 7 Front of oil displacement (blue color) by nanosuspension (red color) at the moment of time 0.3 s for different concentrations of nanoparticles: **a** $\varphi = 0\%$; **b** 0.25%; **c** 0.5%; **d** 1%

continues to flow out in the form of narrow stream. The exit of oil from the micromodel completely stops. At the same time, more than 60% of the volume of model remains saturated with oil. Further waterflooding does not lead to an increase in oil production. The flow getting steady. The steady velocity magnitude contours are shown in Fig. 10. It is clearly seen that the water moves in the form of jets and rivulets.

The oil displacement by nanosuspension occurs in a significantly different way. As shown in Figs. 7, 8 and 9, the movement of nanofluid at high nanoparticle concentrations does not occur in individual rivulets, but in a more uniform front throughout the volume of the computational domain. Nanofluid breaks through to the exit from the model much later than water. Water breaks through to the exit from the model in about 1 second after the start of waterflooding. For a nanofluid (1 wt.%), this time is about 2 seconds. The flow of nanofluid occurs in almost all channels of the micromodel. This is clearly seen from the analysis of the flow velocity distribution (Fig. 10). As a result, nanofluids displace twice the volume of oil compared to water.

The quantitative dependence of the ORF on the time is shown in Fig. 11. As can be seen, with an increase in nanoparticle concentration in the displacing fluid the oil recovery factor increases quite significantly. Thus, in
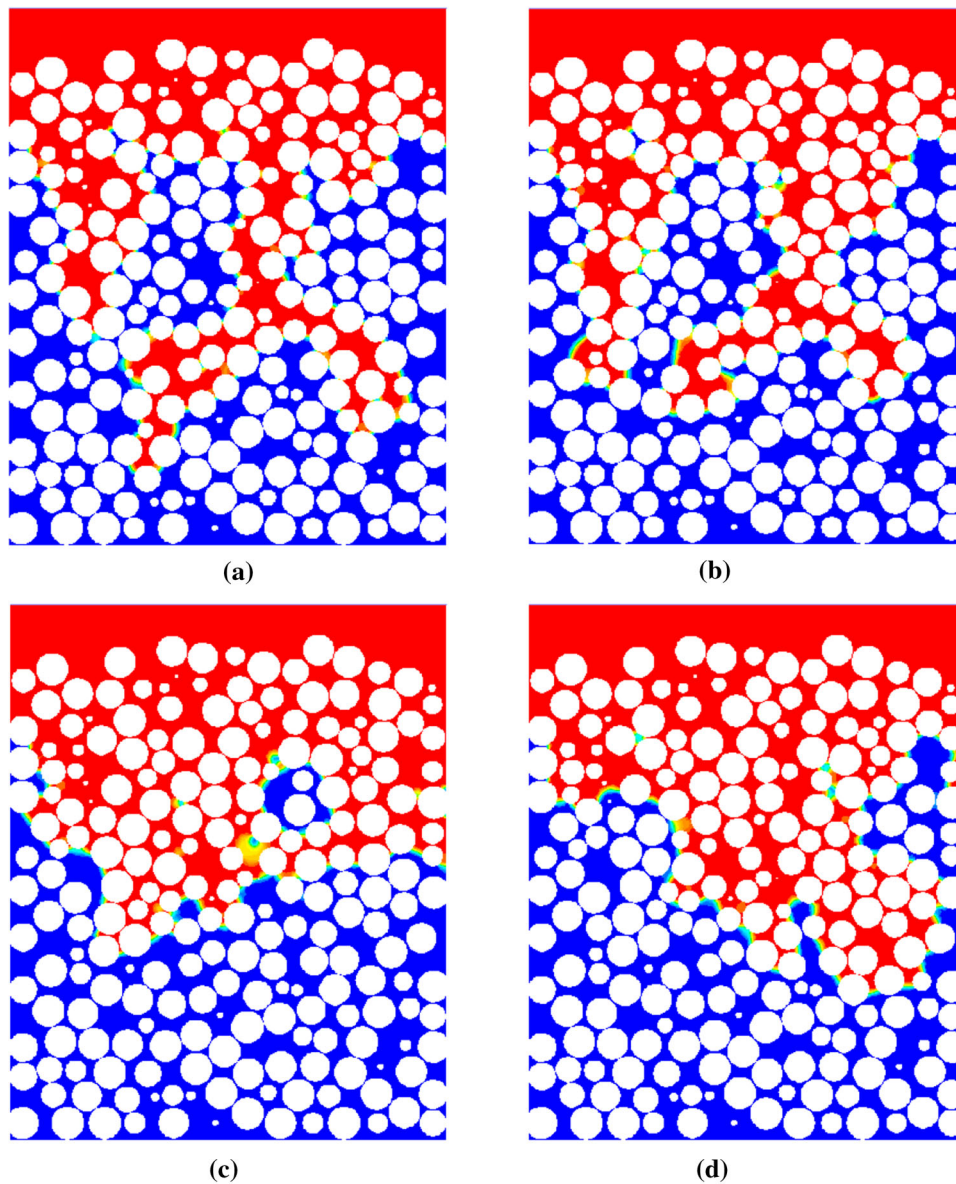
Fig. 8 Front of oil displacement (blue color) by nanosuspension (red color) at the moment of time 0.9 s for different concentrations of nanoparticles: **a** $\varphi = 0\%$; **b** 0.25%; **c** 0.5%; **d** 1%

the course of numerical simulation, it was shown that using the silicon oxide nanosuspension (1 wt.%) allows increasing the ORF almost twice in comparison with distilled water. The oil recovery factor depending on the concentration of particles is given in Fig. 12. It can be seen that the dependence is nonmonotonic. When the concentration of nanoparticles is more than 0.5 wt%, the oil recovery rate is reaching a plateau, and from an economic point of view, it makes no sense to increase the concentration of particles.

Figure 13 shows the time dependence of the pressure drop in the micromodel during oil displacement. As is obvious, the oil displacement process is accompanied by pulsations associated with breakouts of the displacing fluid through the more viscous oil. Once the liquid rushes to the outlet of the computational domain, the pressure drop decreases sharply. At that, the pulsations cease and the pressure drop becomes almost steady. Higher pressure fluctuations are observed at a particle concentration of 0.5 wt%. Experimental data show that at this concentration a minimum of interfacial tension is observed (see Fig. 3). But at the same time, the viscosity of the nanosuspension at this concentration is lower than at a concentration of 1 wt.%. The pressure drop in two-phase flow is determined by the balance between viscous and capillary forces. At the same time, despite
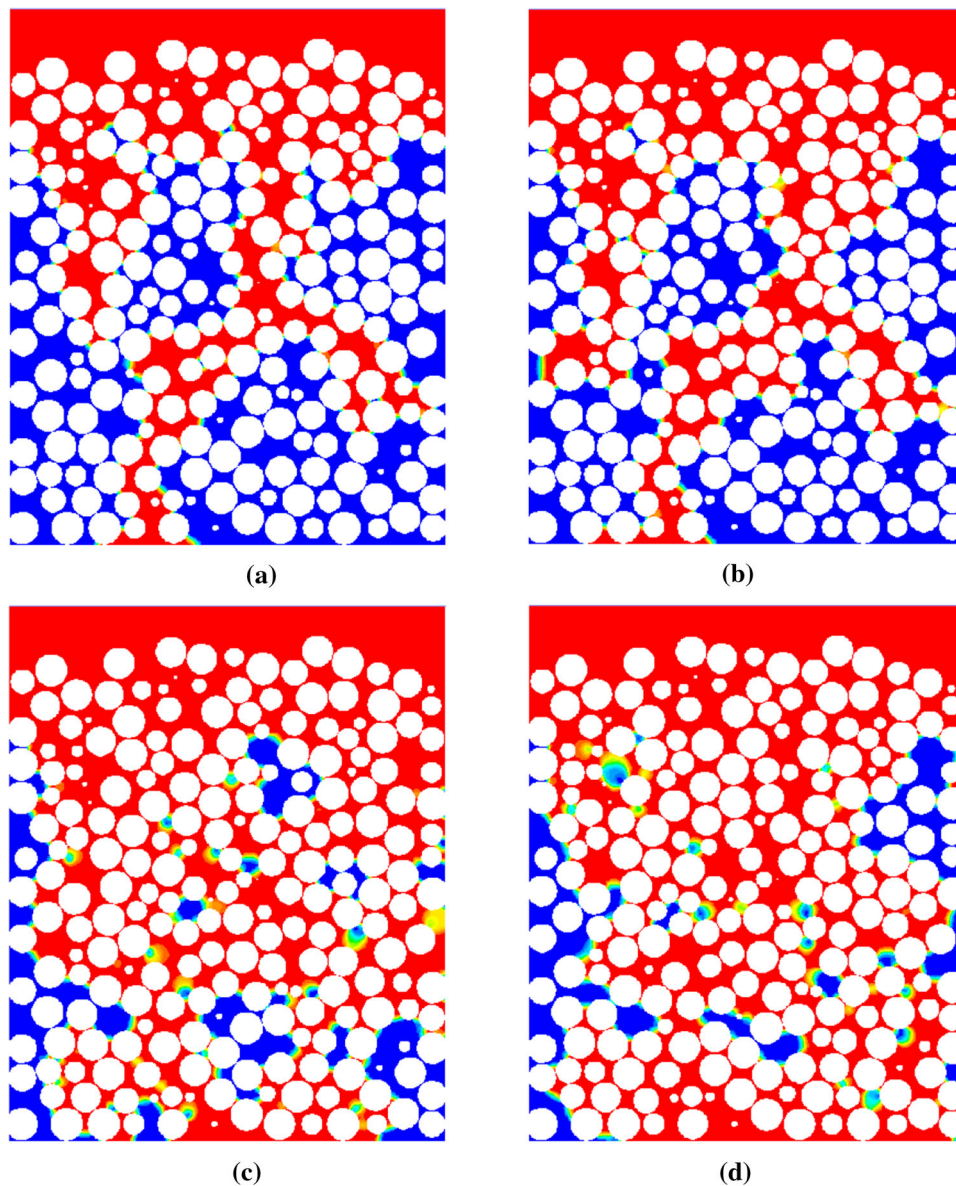
Fig. 9 Front of oil displacement (blue color) by nanosuspension (red color) at the moment of time 5 s for different concentrations of nanoparticles: **a** $\varphi = 0\%$; **b** 0.25%; **c** 0.5%; **d** 1%

the fact that the nanofluid has a higher viscosity and density, the pressure drop for the nanofluid is generally lower than that for pure water. This is due to the fact that, firstly, the nanofluid better wets the surface, secondly, the addition of nanoparticles reduces the interfacial tension, and thirdly, the nanofluid moves almost uniformly throughout the cross section of the computational domain, while the pure water flows in a form of a rivulet through one of the channels in a core, which causes large losses.

To clarify the mechanisms of increasing the oil recovery factor during the reservoir flooding with nanofluid, a systematic study of factors affecting the displacement process efficiency was carried out. Viscosity, interfacial tension and the wetting angle of the displacing fluid were considered as such factors. Each of these parameters varied within wide limits with respect to the water properties, other properties being constant. Thus, the wetting angle varied within the range from 85 to 145° . The relative viscosity of the nanofluid varied from 1 to 4 and the relative IFT coefficient varied from 0.4 to 2.5.

Figures 14 and 15 show the dependence of the ORF on the wetting contact angle. As is seen, the wetting angle has a significant impact on the ORF. Increasing the wetting angle from 85 to 115° increases the ORF
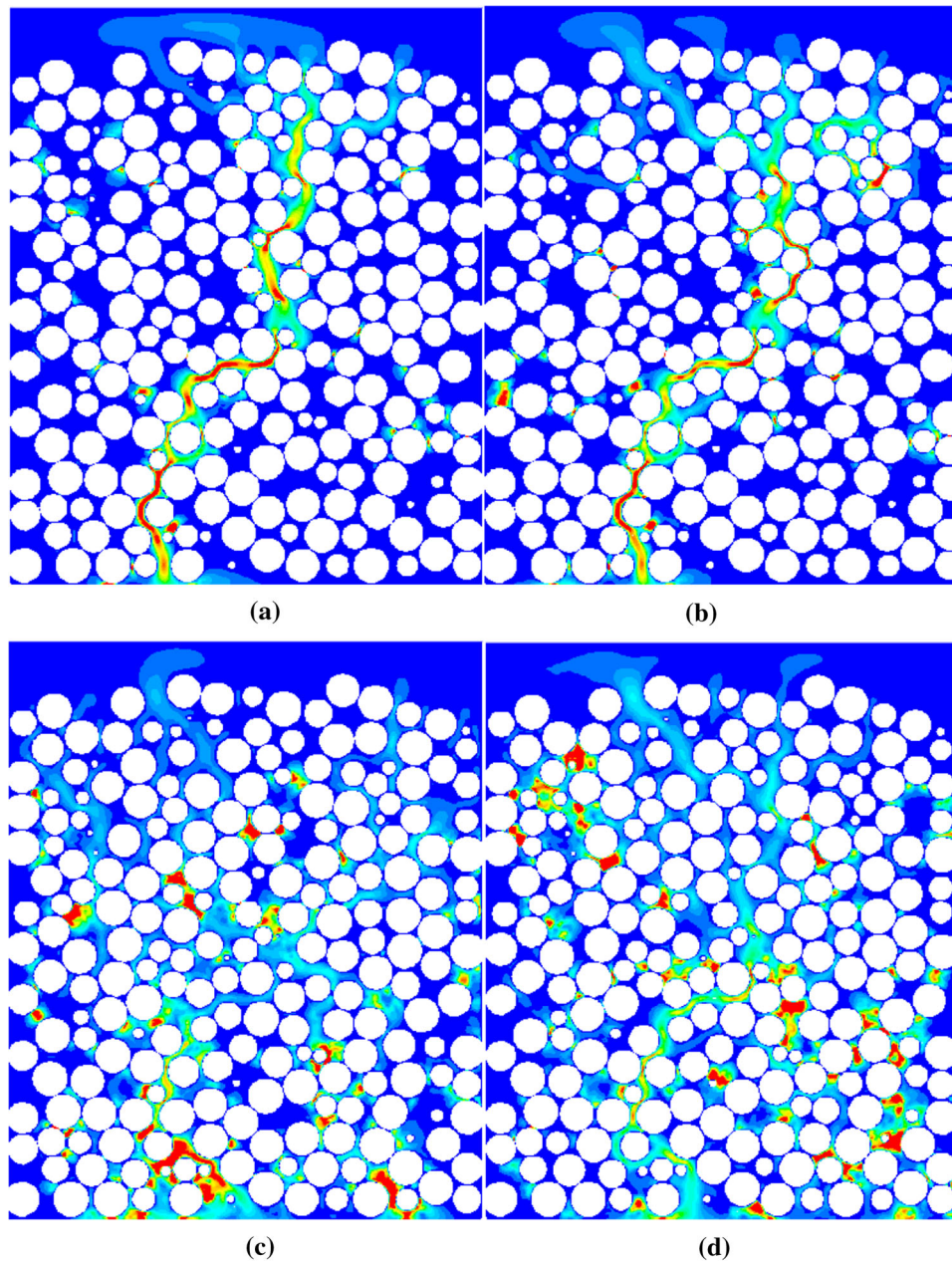
Fig. 10 Contours of mixture velocity magnitude the moment of time 5 s for different concentrations of nanoparticles: **a** $\varphi = 0\%$; **b** 0.25%; **c** 0.5%; **d** 1%

more than twice. At that, the calculations have shown that a further increase in the wetting angle does not result in a further increase in ORF.

Next, the influence of IFT was investigated. Figure 16 shows the dependence of ORF on the relative coefficient of interfacial tension. Here the interfacial tension for water–oil is taken as a unit. Analysis of the results shows that in this case the interfacial tension has a much weaker effect on the ORF than the wetting angle. Thus, with a decrease in the tension coefficient by 6 times, the ORF increases by about 30% (from 0.31 to 0.41).

Figure 17 shows the pressure drop when pumping displacing fluids with different values of interfacial tension with respect to the oil. It was revealed that the pressure drop increases with increasing tension, both at the displacement site and at the site behind the breakthrough of the displacing agent.
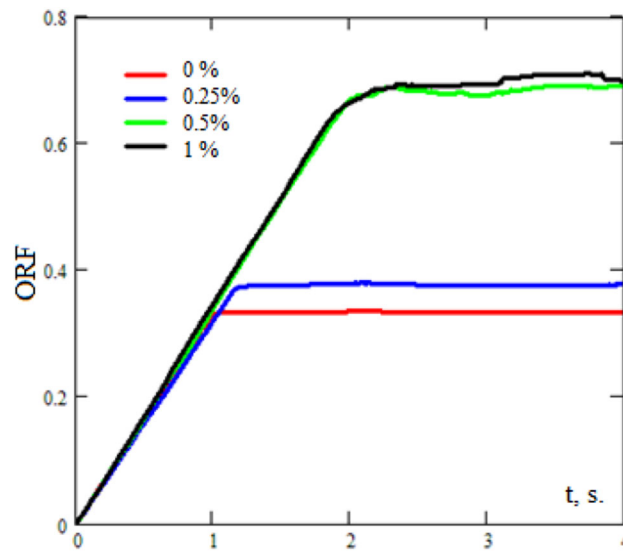
Fig. 11 ORF in the process of oil displacement at different nanoparticles concentrations
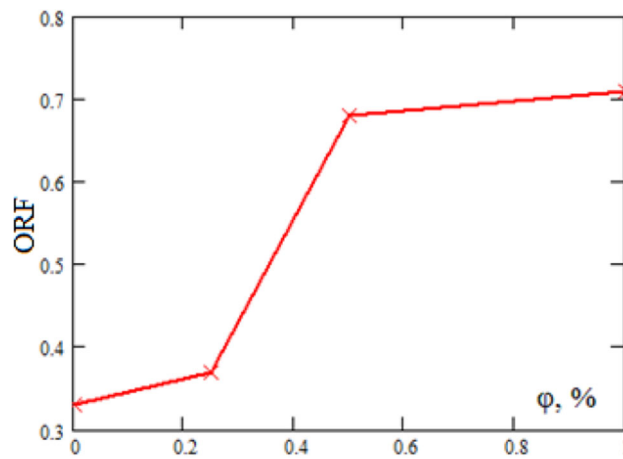

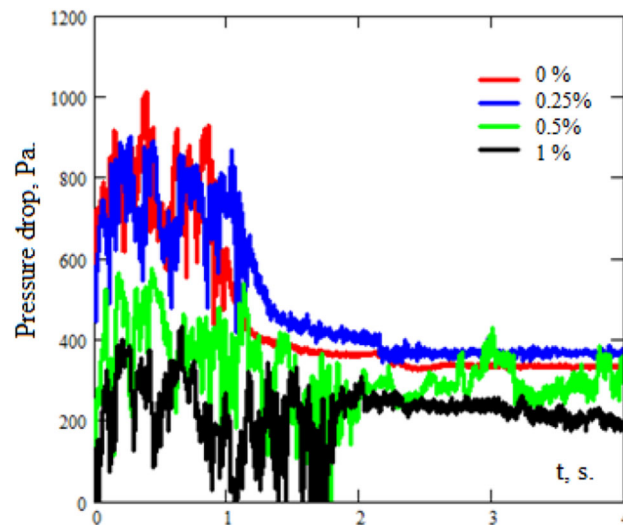**Fig. 12** Oil recovery factor dependence on concentration of nanoparticles

Fig. 13 Pressure drop in the process of oil displacement at different nanoparticles concentrations
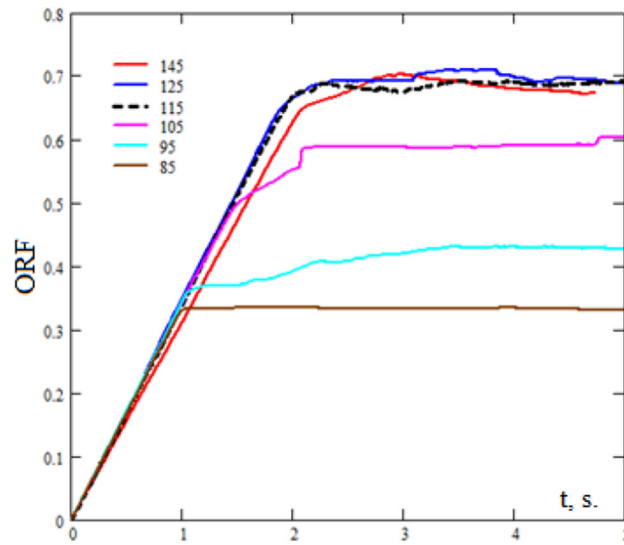
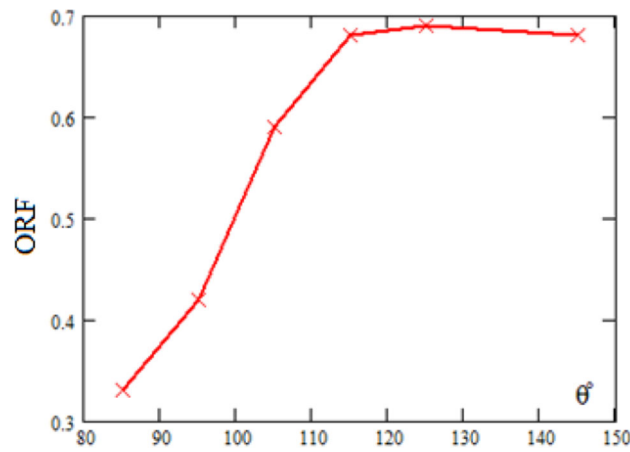**Fig. 14** ORF in the process of oil displacement at different values of contact angles

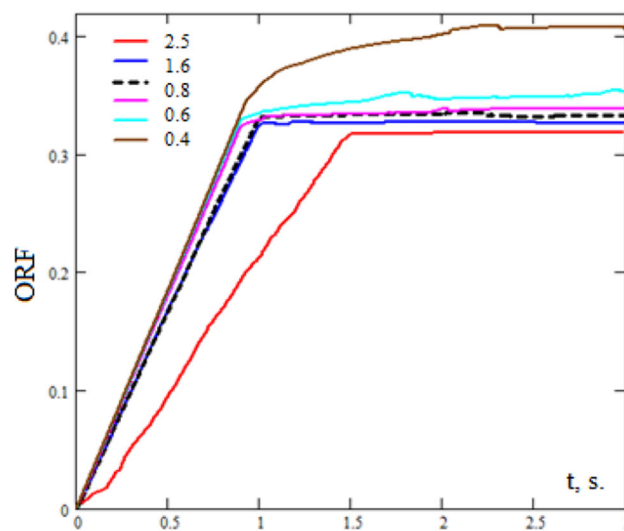**Fig. 15** ORF dependence on value of contact angle

Fig. 16 ORF in the process of oil recovery at different values of the relative IFT coefficient
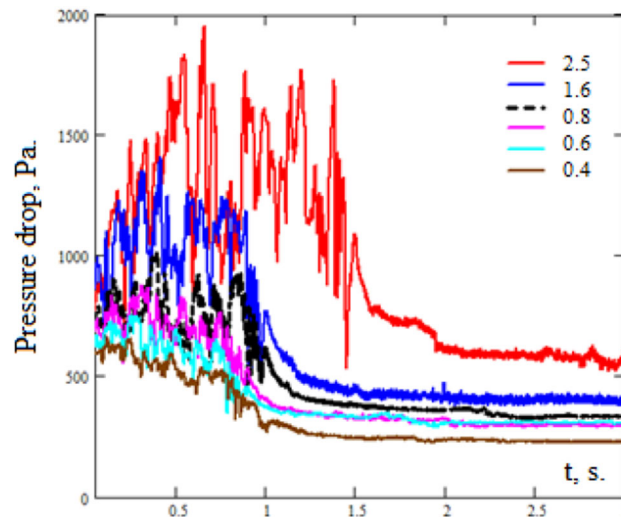
Fig. 17 Pressure drop in the process of oil recovery at different values of the relative IFT coefficient.
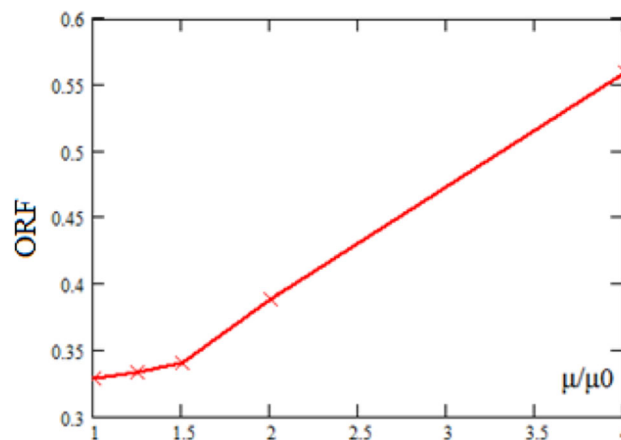

Fig. 18 Oil recovery factor dependence on relative viscosity coefficient of the displacing fluid

Figure 18 shows the dependence of ORF on the relative viscosity coefficient of the displacing fluid. Here the value of water viscosity is taken as a unit. Analysis of the numerical data has shown that the viscosity is the second most important factor after the wetting angle, affecting the ORF. With a fourfold increase in the viscosity coefficient of the displacing liquid, the ORF increased 1.75-fold.

Figure 19 shows the pressure drop when pumping displacing liquids with different relative viscosity. It was revealed that the pressure drop at the displacement site (up to about 1 second) is weakly dependent on the viscosity of the displacing liquid. In this area, the pressure loss is due to surface tension forces. After the liquid breaks through the oil, the pressure loss increases in proportion to the viscosity of the displacing liquid. Thus, in this area the pressure losses are caused, to a greater degree, by hydraulic losses.

As shown by the results of experimental studies presented above, when nanoparticles are added to the displacing liquid, in general, it changes the viscosity, density, interfacial tension and wetting angle. However, since very low concentrations of nanoparticles are used, these changes except for the wetting angle are negligible. Thus, at a nanoparticle concentration equal to 1 wt%, density changes by about 1%, viscosity increases by 10%, while IFT decreases by 10%. Taking into account these data, it becomes clear that such small changes in the liquid parameters could not increase the ORF from 0.32 to 0.71. The only parameter that changed significantly with the addition of nanoparticles was the wetting angle, which increased from 70 to 145°. Thus, in consequence of the analysis of all the data obtained, it was revealed that the main reason for the increase in oil recovery factor when displacing oil by nanosuspension is improved wetting of the core.
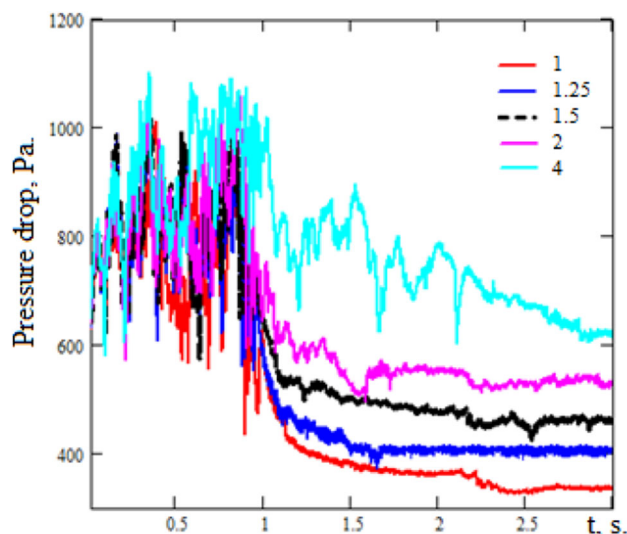
Fig. 19 Pressure drop in the process of oil recovery at different values of the relative viscosity of the displacing fluid

5 Conclusion

A study of the oil displacement process by nanofluids from a 2D microporous model was conducted. Two immiscible liquids flow model and VOF method were used. Experimental data on interfacial tension and the contact angle were used in numerical simulation. For this purpose, systematic experimental studies have been carried out. An aqueous suspension with silicon oxide nanoparticles of an average diameter about 5 nm was used as a nanofluid. The particle concentration varied from 0 to 1 wt. %. As a result of the experiments, it was found that the additive has a significant effect on the wetting angle and slightly affects the interfacial tension.

A computational investigation of the effect of nanoparticle concentration on the efficiency of oil displacement from a porous 2D model was carried out. It is shown that adding silicon oxide nanoparticles (1 wt. %) allows increasing the ORF about 2.15-fold compared to that for water. It was found that as the concentration of particles in the nanosuspension increases the efficiency of oil recovery increases significantly.

To clarify the mechanisms of increasing the ORF during reservoir flooding with nanofluid, a systematic study of factors affecting the efficiency of the displacement process was carried out. Viscosity, interfacial tension and the wetting angle of the displacing fluid were considered as key influencing factors. As a result, it was revealed that the wetting angle has the greatest influence on the ORF. Increasing the wetting angle from 85 to 115° increases the ORF more than twice. At the same time, a further increase in the wetting angle does not lead to a further increase in the ORF. It is shown that the viscosity of the displacing fluid is the second most important factor after the wetting angle, affecting the ORF. It was found that a fourfold increase in the viscosity coefficient of the displacing fluid results in the 1.75-fold increase of ORF. Analysis of the results has shown that the interfacial tension has a much weaker effect on the ORF. Thus, a sixfold decrease in tension coefficient (at the interface between oil and displacing liquid) leads to about 1.3-fold increase in ORF.

When adding nanoparticles to the fluid with a concentration of 1 wt. % the density changes by about 1%, viscosity increases by 10%, while IFT decreases by 10%. Taking into account the above data, it becomes clear that such small changes in the fluid properties could not increase the ORF from 0.32 to 0.71. The only parameter that has changed significantly with the addition of nanoparticles was the wetting angle, which increased from 70 to 145°. Thus, in consequence of the analysis of all the data obtained, it was revealed that the improvement of rock wetting is the main factor for the increase in oil recovery at the oil displacement by a nanofluid.

References

1. Brackbill, J.U., Kothe, D.B., Zemach, C.: A continuum method for modeling surface tension. J. Comput. Phys. **100**(2), 335–354 (1992)
2. Ehtesabi, H., Ahadian, M.M., Taghikhani, V.: Enhanced heavy oil recovery using TiO2 nanoparticles: investigation of deposition during transport in core plug. Energy Fuels **29**(1), 1–8 (2015)
3. Hirt, C.W., Nichols, B.D.: Volume of fluid (VOF) method for the dynamics of free boundaries. J. Comput. Phys. **39**(1), 201–225 (1981)
4. Hu, Z., Siddeequah, M.A., Ghulam, R., Paul, W.J.G., Dongsheng, W.: Nanoparticle-assisted water-flooding in Berea sandstones. Energy Fuels **30**(4), 2791–2804 (2016)
5. Karimi, A., Fakhroueian, Z., Bahramian, A., Pour, Khiabani, N., Darabad, J.B., Azin, R., Arya, S.: Wettability alteration in carbonates using zirconium oxide nanofluids EOR implications. Energy Fuels **26**(2), 1028–1036 (2012)
6. Kistler, S.F.: Hydrodynamics of wetting. In: Berg, J.C. (ed.) Wettability, pp. 311–429. Marcel Dekker, New York (1993)
7. Kokal, S., Al-Kaabi, I.A.: Enhanced oil recovery: challenges & opportunities. World Petroleum Council: Official Publication **2010**, 64–69 (2010)
8. Li, S., Hendraningrat, L., Torsaeter, O.: Improved oil recovery by hydrophilic silica nanoparticles suspension: 2 phase flow experimental studies. In: Proceedings of the IPTC 2013: International Petroleum Technology Conference; European Association of Geoscientists & Engineers, Beijing, China, 26–28 March 2013 (2013)
9. Maes, J., Soulaine, C.: A new compressive scheme to simulate species transfer across fluid interfaces using the Volume-Of-Fluid method. Chem. Eng. Sci. **190**, 405–418 (2018)
10. Mcelfresh, P.M., Holcomb, D.L., Ector, D.: Application of nanofluid technology to improve recovery in oil and gas wells. In: SPE International Oilfield Nanotechnology Conference and Exhibition. Society of Petroleum Engineers, SPE154827 (2012)
11. Minakov, A.V.: Numerical algorithm for moving-boundary fluid dynamics problems and its testing. Computational Mathematics and Mathematical Physics **54**(10), 1560–1570 (2014)
12. Minakov, A.V., Shebeleva, A.A., Yagodnitsyna, A.A., Kovalev, A.V., Bilsky, A.V.: Flow regimes of viscous immiscible liquids in T-type microchannels. Chem. Eng. Technol. **42**(5), 1037–1044 (2019)
13. Minakov, A.V., Pryazhnikov, M.I., Suleymana, Y.N., Meshkova, V.D., Guzei, D.V.: Experimental study of nanoparticle size and material effect on the oil wettability characteristics of various rock types. J. Mol. Liq. **327**, 114906 (2021)
14. Roustaei, A., Bagherzadeh, H.: Experimental investigation of SiO2 nanoparticles on enhanced oil recovery of carbonate reservoirs. J. Pet. Explor. Prod. Technol. (2014). https://doi.org/10.1007/s13202-014-0120-3
15. Roustaei, A., Bagherzadeh, H.: Experimental investigation of SiO2 nanoparticles on enhanced oil recovery of carbonate reservoirs. J. Pet. Explor. Prod. Technol. **5**, 27–33 (2015)
16. Rudyak, V.Y., Minakov, A.V., Smetanina, M.S., Pryazhnikov, M.I.: Experimental data on the dependence of the viscosity of water- and ethylene glycol-based nanofluids on the size and material of particles. Dokl. Phys. **61**(3), 152–154 (2016)
17. Stosur, G.J.: SPE 84864 EOR: Past, Present and What the Next 25 Years May Bring. In: SPE International Improved Oil Recovery Conference in Asia Pacific, 20-21 October 2003, Kuala Lumpur, Malaysia (2003)
18. Suleimanov, B.A., Ismailov, F.S., Veliyev, E.F.: Nanofluid for enhanced oil recovery. J. Pet. Sci. Eng. **78**(2), 431–437 (2011)
19. Thomas, S.: Enhanced Oil Recovery—An Overview. Oil & Gas Science and Technology—Rev. IFP, 63, 19-19 (2008)
20. Tunio, S.Q., Tunio, A.H., Ghirano, N.A., El Adawy, Z.M.: Comparison of different enhanced oil recovery techniques for better oil productivity. Int. J. Appl. Sci. Technol. **1**(5), 143–153 (2011)
21. Wasan, D.T., Nikolov, A.D.: Spreading of nanofluids on solids. Nature **423**, 156–159 (2003)